crystals

MDPI

Article

Research on Corrosion Resistance and Formation Mechanism of Molybdate Composite Film

Yi Wan [1], Qiaoping Liu [2] and Yunying Fan [1,*]

[1] Faculty of Materials Science and Engineering, Kunming University of Science and Technology, Kunming 650093, China
[2] Shandong Special Equipment Inspection Research Institute, Linyi 276000, China
* Correspondence: fanyunying2022@163.com

Abstract: In order to reduce phosphorus pollution, the low phosphorus passivation process on Q235 steel was studied. The electrochemical method was used to test the corrosion resistance of sodium molybdate low phosphorus passivation. The polarization curve shows that the corrosion current of the sample passivated by low phosphorus is only 1/4 of that of the blank sample. Under scanning electron microscopy, the passivation film obtained by low phosphorus passivation treatment had the lowest phosphorus content and was more uniform and compact. The XPS (X-ray photoelectron spectroscopy) and OCP (open circuit potential) were used to study the film formation regularity and mechanism of low molybdenum sodium passivation. The results show that sodium molybdate low phosphorus passivation film has good corrosion resistance. The formation process of a passivation film can be divided into four stages alternating phosphating and passivation. The surface of the passivation film is mainly composed of phosphate, molybdate, molybdenum oxide, and their crystalline hydrates. The low phosphorus passivation process of sodium molybdate can reduce the concentration of phosphorus ions and reduce its pollution to the environment, which has broad application prospects.

Keywords: molybdenum compound; low phosphorus passivation; corrosion resistance; film formation mechanism

check for updates

Citation: Wan, Y.; Liu, Q.; Fan, Y. Research on Corrosion Resistance and Formation Mechanism of Molybdate Composite Film. *Crystals* **2022**, *12*, 1559. https://doi.org/10.3390/cryst12111559

Academic Editor: Ludmila Isaenko

Received: 20 September 2022
Accepted: 28 October 2022
Published: 1 November 2022

1. Introduction

Coating protection is a common anticorrosion technology for iron and steel materials [1]. In order to remove the oxide scale and oil stain on the steel surface, a series of pretreatment shall be carried out on the steel substrate before coating, including acid pickling, alkali washing, grinding, etc. [2]. Each step of these processes needs to be washed at least twice to ensure a smooth surface and prepare for the subsequent coating. After pickling and washing, the surface of the steel matrix was left in weak acid and a wet state for a long time, which makes it easy to begin corrosion again and loose corrosion products are formed on the surface. In the subsequent coating process, the adhesion and corrosion resistance of the coating will be affected [3].

In order to solve the above problems, it is necessary to pretreat the steel before coating and form a protective film on its surface. This dense, protective film can effectively prevent rust returning before steel coating, which is an important process in the coating processing [4].

Phosphating is the most widely used process in the pretreatment of steel coating, which forms a layer of phosphating film on the surface of steel. Phosphating treatment has the advantages of low cost, simple operation, and good corrosion resistance, but phosphating will cause great pollution to the environment [5,6]. In order to solve the problem of environmental pollution, people began to try to replace the phosphating process. At present, zirconium film and silane conversion film are more studied. However, the corrosion resistance and adhesion of zirconated film are far lower than that of phosphate

film, and the film-forming rate is slow, and the self-healing ability is poor [7]. The solution stability of silane conversion film technology is poor, the film is thin, and the corrosion resistance is also lower than that of phosphating film [8].

In order to maintain the excellent corrosion resistance of phosphating treatment and reduce the harm of phosphating to the environment, the low phosphorus passivation process of sodium molybdate was studied. The passive film with corrosion resistance was prepared by reducing the amount of phosphate, and the film formation mechanism was determined.

2. Experimental Procedure

2.1. Experimental Materials

Q235 carbon steel is used as the base material, and the specification is 50 mm × 40 mm × 1 mm, all chemical reagents used are analytical pure raw materials. The composition of Q235 carbon steel is shown in Table 1.

Table 1. Composition of Q235 carbon steel material.

Chemical Element	C	Si	Mn	S	P	Cr	Ni	Cu	Fe
Element (%)	0.12–0.20	≤0.3	0.30–0.70	≤0.045	≤0.045	≤0.30	≤0.30	≤0.30	≥99.97

2.2. Preparation of Low Phosphorus Passivation Solution Material

The base material was defatted on the surface and washed after chemical pickling. The substrate was activated for 7–10 s in a 10% HCl solution and continued to be washed. The Q235 steel sample was impregnated in passivation solution for 60 s by impregnation method, and then dried at a constant temperature of 100 °C. The desired passivated sample was obtained.

In order to explore the performance difference between low phosphorus passivation and traditional phosphating technology, the comparison groups of low phosphorus passivation and traditional phosphating technology [9] was set, as shown in Tables 2 and 3.

Table 2. Low phosphorus passivated solution formula.

	Na_2MoO_4	Na_3PO_4	H_3BO_3	H_2O
Content (g/L)	2.5	1	3 mL/L	Constant volume to 1 L

Table 3. Conventional phosphated sample solution formula.

	ZnO	$C_6H_8O_7$	H_3PO_4	$NaNO_2$	H_2O
Content (g/L)	15	1.5	50 mL/L	10 mL/L	Constant volume to 1 L

2.3. Characterisation

Nova-Nano450 field emission scanning electron microscope (SEM) and energy dispersive spectrometer was used for micromorphology analysis and detection of the samples. The surface of the material was observed. PHI5000 VersaProbe X-ray photoelectron spectroscopy (XPS) was used to measure the content and distribution depth of elements on passivation film.

An electrochemical workstation (CHI660E) was used to obtain electrochemical polarization curves, open circuit potential curves, and electrochemical impedance spectroscopy in 3.5 wt% NaCl solution, and the corrosion protection performance of different samples was observed in air. The traditional three-electrode cell was used in the experiment, and

the sample was used as the working electrode (1 cm × 1 cm). In addition, a 2 cm × 2 cm platinum plate and saturated calomel electrode were used as the counter and reference electrode, respectively. The scanning rate was 0.5 mVs^{-1}, and the potential range was −3.5 V to 2 V vs. SCE (saturated calomel electrode).

3. Results and Discussion

3.1. Electrochemical Workstation

Figure 1 shows a plot of the Eop versus time of the sample in a 3.5% NaCl solution. The unpassivated sample was in the process of constant negative shift. The traditional phosphating sample and low phosphorus passivation sample stabilized after a rapid negative shift. The value at 1800 s was taken as an open circuit potential, and the E_{op} was −0.685 V, −0.576 V, and−0.538 V. Measured open circuit potential under actual corrosion conditions can characterize the thermodynamic trends of metal electrochemical corrosion. The positive shift of the open circuit potential indicates a reduced corrosion tendency of the metal [10]. It can be seen that the corrosion tendency of the low phosphorus passivation process is smaller than that of the traditional phosphating process.

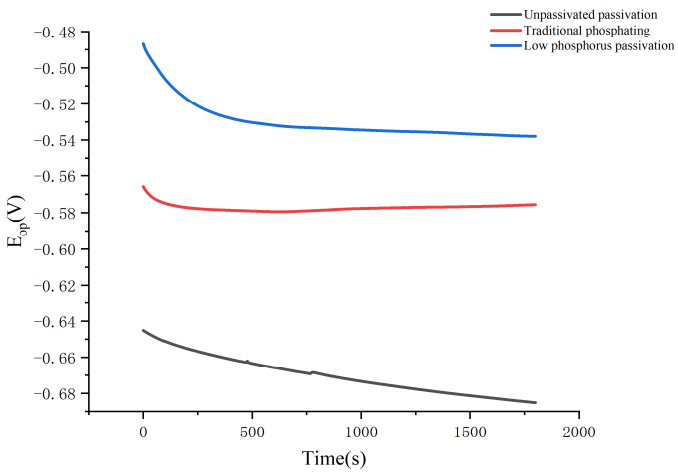

Figure 1. Open circuit potential of the three samples in a 3.5% NaCl solution.

The relationship between the metal corrosion rate and the corrosion current can be expressed by the following formula:

$$V = \frac{I_{\mathrm{corr}} M}{\mathrm{nFS}} \tag{1}$$

V is corrosion rate (mm/y); Icorr is corrosion current (mA); M is the relative atomic mass of the metal atom; n is the valence of metal; F is Faraday's constant; S is the sample area (mm^2) [9].

Figure 2 shows the electrochemical polarization curves of the Q235 steel samples in 3.5% NaCl solution after nonpassivation, conventional phosphatizing, and low phosphatizing. The polarization curve was tested from open circuit potential, and the fitting data obtained after fitting Tafel curve was shown in Table 4.

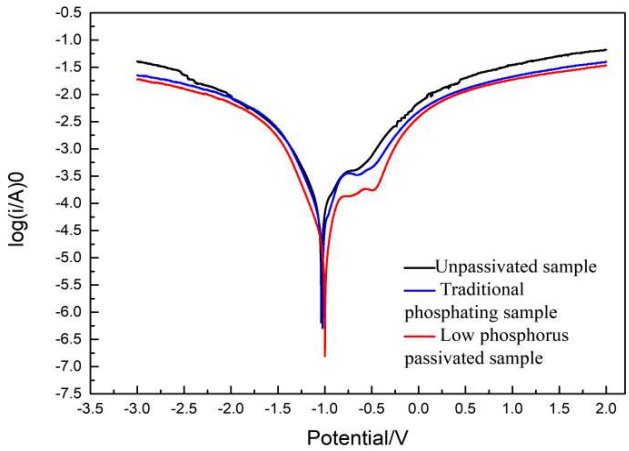

Figure 2. Electrochemical polarization curves of Q235 steel samples by different treatment methods in 3.5% NaCl solution.

Table 4. Corrosion electrochemical parameters of unpassivated passivation, low phosphorus passivation, and traditional phosphating of Q235 steel samples in 3.5% NaCl solution.

Sample Status	*E* Corr /V	*I* Corr × 10^{-4}/mA
Unpassivated sample	−1.038	6.45
Conventional phosphating sample	−1.025	5.19
Low phosphorus passivated sample	−0.999	1.536

The level of the corrosion current is directly related to the corrosion rate of the material in the medium [10]. It can be seen from Equation (1) that the corrosion rate is proportional to the corrosion current under the same conditions [11]. According to Formula (1), the change of the corrosion rate is proportional to the corrosion current when other variables are kept unchanged. The smaller the corrosion current, the lower the corrosion rate that can be obtained after substituting into the formula. The corrosion rate can reflect the effect of the passivation film. Therefore, the lower the corrosion current of the composite film, the better the corrosion resistance. It can be seen from Figure 2 and Table 4 that the corrosion current of the low phosphorus passivated Q235 steel sample is significantly smaller than that of the unpassivated sample and the traditional phosphating sample. Through calculation, compared with the unpassivated sample, the traditional phosphating sample has a corrosion inhibition efficiency of 19%, while the low phosphorus passivated sample has a corrosion inhibition efficiency of 76% compared with the unpassivated sample. The low phosphorus passivation sample and traditional phosphating sample have a passivation zone in the −1.0 V to −0.5 V range. It can be clearly seen from Figure 1 that the potential range of the passivation zone is the largest in the low phosphorus passivation sample, followed by the traditional phosphating sample [12,13]. It shows that the passivation film of the low phosphorus passivation sample has better corrosion resistance.

To confirm the results of the polarization curve, the electrochemical impedance spectrum (EIS) is a common test method, used to test the corrosion resistance of the protective film. The electrode of the corrosive original cell is disturbed by the signal of a small AC current or voltage to obtain the AC impedance information data of the tested sample electrode.

Figure 3a shows that the shapes of the three samples, unpassivated passivation, low phosphorus passivation, and traditional phosphating process, are basically similar and the difference starts in the low frequency region. The tolerance radian of low phosphorus passivation sample in the high frequency region was significantly higher than that in the other two samples [14], which confirms that the low phosphorus passivation sample has better corrosion resistance on Q235 steel than the traditional phosphating sample. This is

consistent with the results shown by the polarization curve. Figure 3b shows the curves of the phase angle versus frequency relationship when the three samples were tested in EIS. It can be seen that the phase angle of the low phosphorus passivation sample is greater than that of the traditional phosphorylated samples and the unpassivated sample. This indicates that the passivation membrane formed by the low phosphorus passivation sample has better integrity and can effectively inhibit the penetration of the corrosion ions to the substrate [15]. The impedance data were fitted to draw the equivalent circuit in Figure 3c. Rs represents the solution resistance; Rp represents the charge transfer resistance; CPE is the double-layer capacitor. The fitting results are listed in Table 5.

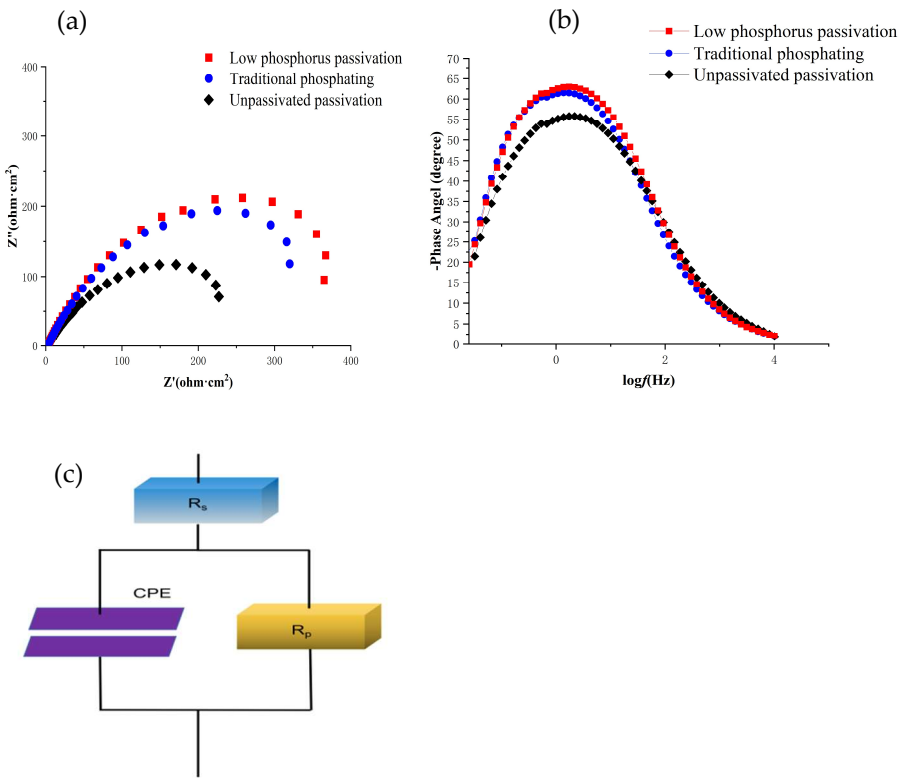

Figure 3. (**a**) Electrochemical impedance spectroscopy of passive film formed by Q235 steel by different treatment methods in 3.5% NaCl solution; (**b**) phase angle vs. frequency; (**c**) EIS equivalent circuit.

Table 5. EIS parameters fitted by the equivalent circuit proposed in Figure 3c.

	Rs (Ω cm^2)	Rp (Ω cm^2)	CPE (μF cm^{-2})
Unpassivated sample	2.175	417.6	585.44
Conventional phosphating sample	2.506	659	475.53
Low phosphorus passivated sample	2.398	701	407.33

Generally, higher values of Rp represent lower electron transfer efficiency between metal and electrolytes. Table 5 shows that the values of the low phosphorus passivated sample are greater than those of the conventional phosphating sample and the unpassivated sample. It shows that the low phosphorus passivation sample has better corrosion resistance.

3.2. Micromorphology Analysis and Detection

The surface microstructure of Q235 steel without passivation, traditional phosphating, and low phosphorus passivation was tested by SEM, and the results are shown in Figure 4.

To verify the existence of the film, the cross section of the sample was tested by scanning electron microscopy.

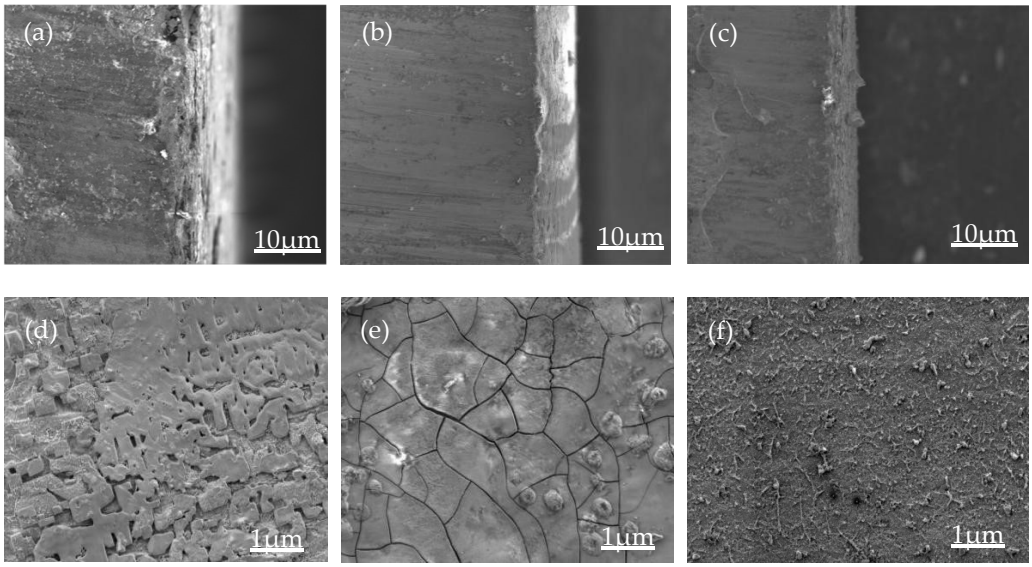

Figure 4. Surface micromorphology of Q235 steel sample in 3.5% NaCl solution. (**a**) SEM micrograph of cross section of unpassivated sample. (**b**) SEM micrograph of cross section of traditional phosphating sample. (**c**) SEM micrograph of cross section of low phosphorus passivated sample. (**d**) SEM micrograph of the surface of unpassivated sample. (**e**) SEM micrograph of the surface of traditional phosphating sample. (**f**) SEM micrograph of the surface of low phosphorus passivated sample.

Figure 4a is the scanning electron microscope image of the section of the unpassivated sample. It can be seen that there is no obvious dividing line between the surface and section of the steel sheet, which belongs to the same material and has no film layer. In Figure 4b,c, obviously bright phosphorus element appears in the cross sections, from which it can be inferred that the passivation film containing phosphorus element is obtained. In Figure 4c, the phosphorus content is significantly less, and the surface of the film is relatively uniform. Then, the surface of the steel sheet was tested by scanning electron microscopy, the surface of the unpassivated sample was uneven and there were many fine cracks on the surface, which would be easily corroded (Figure 2d). Figure 4e shows the sample after the traditional phosphating process, a passivation film is formed on the surface of the sample, but the film cannot completely cover the matrix. After low phosphorus passivation, a dense passivation film can be formed on the surface of the Q235 steel matrix, which completely covers the matrix and can effectively prevent corrosion caused by the combination of the matrix and oxygen in the air. Due to the addition of molybdenum salt, there is an irregular, fine granular structure in the passivation film, which can effectively prevent the charge transfer in the process of electrochemical corrosion, so as to achieve an excellent anticorrosion effect (Figure 4f) [16].

In conclusion, it was proved that the sample forms a passivation film attached to the surface.

To demonstrate that the low phosphorus passivation membrane contains the Mo and P elements, the EDS test was examined for the components of the low phosphorus passivation membrane.

Figure 5 shows that the main elements composing the passivation membrane are Fe, O, Mo, and P. The presence of Mo and P elements suggests the involvement of molybdate and phosphate in the membrane-forming reaction. The large presence of iron in the passivation membrane indicates that the membrane formed by the low phosphorus passivation process is dominated by Fe. The oxide film formed in the air and sodium molybdate both contain O elements, so the oxygen element content in the passivation film is also relatively large.

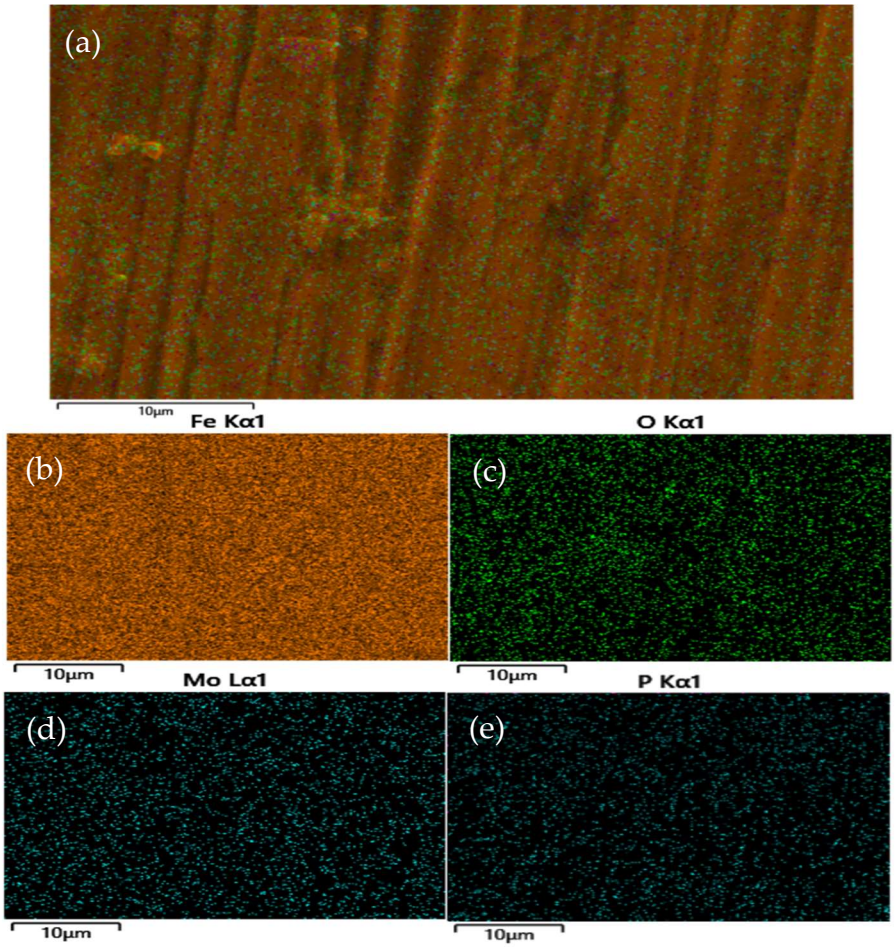

Figure 5. Energy dispersive spectrometer of low phosphorus passivation sample; (**a**) is the total energy dispersive spectrometer; (**b**) is the energy dispersive spectrometer of Fe; (**c**) is the energy dispersive spectrometer of O; (**d**) is the energy dispersive spectrometer of Mo; (**e**) is the energy dispersive spectrometer of P.

3.3. X-ray Photoelectron Spectroscopy

In order to further prove that the passivation film contains phosphorus and other elements and explore the components of the passivation film, the sample passivated with low phosphorus was characterized by X-ray photoelectron spectroscopy (XPS).

The XPS narrow scan spectrum of the three main film-forming elements was peak-fitting, and the results are shown in Figure 6. It can be seen from Figure 6a that there are mainly two kinds of valence oxygen elements under the spectrum peak. Table 6 shows their binding energies are 531.2 eV and 533.2 eV (Table 6), respectively, corresponding to the oxygen elements in MoO_4^{2-} molybdenum bond and the oxygen elements in adsorption water or crystal water. Figure 6b shows that there are two valence phosphorus elements under the peak of phosphorus spectrum, and their binding energies are 133 eV and 133.79 eV, respectively, corresponding to the P element in HPO_4^{2-} and the P element in PO_3^{3-}. There are mainly three valence molybdenum elements under the spectral peak, and their binding energies are 232.3 eV, 232.87 eV, and 235.77 eV (Table 6), respectively, corresponding to the molybdenum elements in water of molybdate crystal, molybdate, and molybdenum oxide [17]. It can be seen that the passivation film is mainly composed of phosphate, molybdate, their crystalline hydrate, and oxides of molybdenum (Figure 6c).

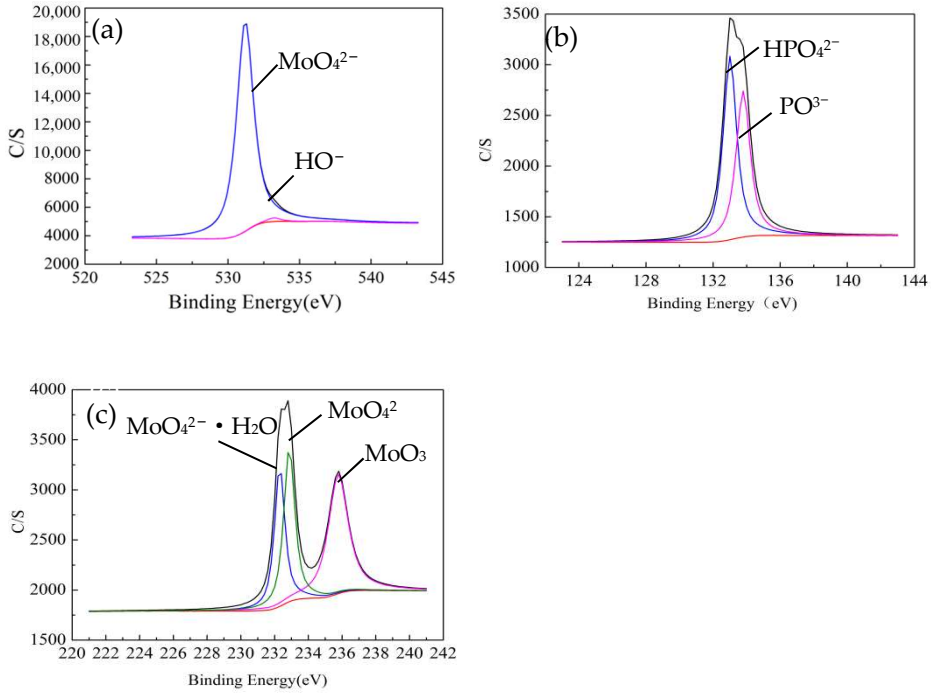

Figure 6. The high-resolution XPS spectrum of (**a**) O2p, (**b**) P2p, and (**c**) Mo2p.

Table 6. Element-binding energy and percentage content of passivation film.

Chemical Element	Mo3d	P2p	O1s
Elemental binding energy/eV	232.3/235.77/235.87	133/133.79	531.2/533.2
Percentage composition/at%	6.9	4.6	41.5

3.4. Explore the Mechanism of Molybdate Passivation

According to the results of the EDS and XPS tests, the reaction process of the low phosphorus passivation process was speculated.

Figure 7a shows that when the Q235 steel is immersed in the low phosphorus passivation solution the main film-forming components present in the passivation solution are PO_4^{3-}, H^+, O^{2-}, and MoO_4^{2-}.

Figure 7b shows the metal iron is in contact with the passivation solution and the metal anode dissolves, the cations accumulate due to the slow diffusion rate and form a very thin oxide film, which is composed of ferrous oxide. The phosphate root is hydrolyzed in an aqueous solution, and the products are PO_4^{3-}, HPO_4^{2-}, and H_3PO_4.

Figure 7c shows that since the composition of the surface HBO_3 has the ability to bind the OH- in the water molecules, the H^+ concentration in the solution increases. Effectively promoted the oxidation of partial Fe^{2+} to Fe^{3+}. Fe^{2+} binds to HPO_4^{2-} and PO_4^{3-} to generate phosphorylated membranes insoluble in water. Fe^{3+} binds to MoO_4^{2-} and O^{2-} to form a stable sediment attached to the body surface. It is also speculated that sodium molybdate and water form molybdenum trioxide hydrate under acidic conditions. After drying, the hexavalent oxides of molybdenum are stably attached to the steel matrix surface [18].

Figure 7d shows the molybdate low phosphorus passivation membrane is composed of Fe_3 $(PO_4)_2$ [19] and Fe_2O_3 + Fe_2 $(MoO_4)_3$ [20]. The reaction mechanism is as Equations (2)–(6):

$$Fe^{2+} + PO_4^{3-} + H^+ = FeHPO_4\downarrow \quad (2)$$

$$Fe^{2+} + HPO_4^{2-} = FeHPO_4 \downarrow \quad (3)$$

$$3FeHPO_4 = Fe_3(PO_4)_2\downarrow + H_3PO_4 \quad (4)$$

$$4Fe^{3+} + 3MoO_4^{2-} + 3O^{2-} = Fe_2O_3 \downarrow + Fe_2\ (MoO_4)_3\downarrow \quad (5)$$

$$MoO_4^{2-} + H_2O + 2H^+ = MoO_3 \cdot 2H_2O \quad (6)$$

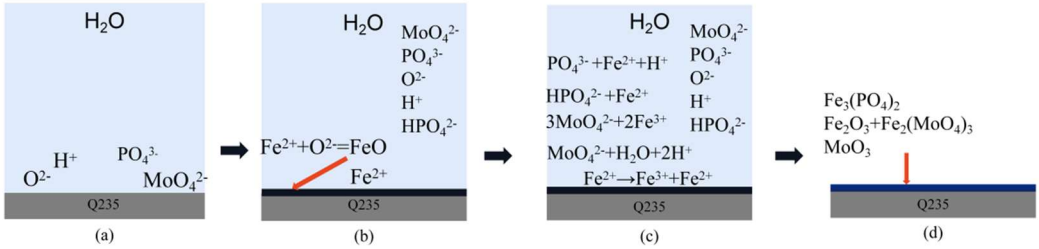

Figure 7. Reaction process of Q235 steel in low phosphorus passivation solution; (**a**) The matrix was just immersed into the passivation solution; (**b**)The matrix surface produces a layer of FeO passivation membrane and phosphate hydrolysis; (**c**) Fe^{2+} and Fe^{3+} on the surface of the matrix react with the ions in the passivation fluid; (**d**) The formed passivation film is dried and then adsorbed to the matrix surface.

4. Conclusions

(1) A new low phosphorus passivation solution was prepared on the basis of traditional phosphating, which significantly reduced the environmental pollution caused by phosphate.

(2) In a 3.5% NaCl solution, open circuit potential shows the positive shift in molybdate low phosphorus passivation. The polarization curve shows significant passivation regions with the self-corrosion current being the smallest of the three sample. Electrochemical impedance spectroscopy shows that the arc resistance of the low phosphorus passivation and the traditional phosphating sample in the low frequency region is significantly greater than that of the unpassivation sample, indicating that the resulting passivation film produced can effectively inhibit the charge transfer during corrosion. Moreover, the tolerance radian of the molybdate low phosphate passivation sample is greater than that of the traditional phosphating sample, indicating that the molybdate low phosphorus passivation process can effectively improve the corrosion resistance of the matrix.

(3) The membrane formation mechanism of low phosphorus passivation of molybdate was explored by EDS and XPS. The main component of the passivation film is composed of Fe_2O_3 + Fe_2 $(MoO_4)_3$, MoO_3, and Fe_3 $(PO_4)_2$. Under the SEM observation, the molybdate low phosphate passivation film is more dense than the phosphating film, and it has a better corrosion resistance effect.

Author Contributions: Conceptualization, Y.F.; methodology, Y.F. and Y.W.; software, Y.W.; validation, Y.F. and Y.W.; investigation, Y.F., Y.W.; resources, Q.L.; writing—original draft preparation, Y.W.; writing—review and editing, Y.F. and Y.W. All authors have read and agreed to the published version of the manuscript.

Funding: This research received no external funding.

Institutional Review Board Statement: Not applicable.

Informed Consent Statement: Not applicable.

Data Availability Statement: Not applicable.

Conflicts of Interest: The authors declare no conflict of interest.

References

1. Yu, Z.; Hu, J.; Meng, H. A Review of Recent Developments in Coating Systems for Hot-Dip Galvanized Steel. *Front. Mater.* **2020**, *7*, 74. [CrossRef]
2. Matsumoto, S.; Yamaga, S.; Yoshikawa, A. New surface passivation method for GaAs and its effect on the initial growth stage of a heteroepitaxial ZnSe layer. *Appl. Surf. Sci.* **1992**, *60*, 274–280. [CrossRef]
3. Ming, J.; Shi, J.; Sun, W. Effects of Mill Scale and Steel Type on Passivation and Accelerated Corrosion Behavior of Reinforcing Steels in Concrete. *J. Mater. Civ. Eng.* **2020**, *32*, 4020029. [CrossRef]

4. Zhao, Y. Interaction Mechanism between Zn and Passivated Stainless Steel. *Int. J. Electrochem. Sci.* **2019**, *14*, 301–314. [CrossRef]
5. Park, J.H.; Bolan, N.S.; Chung, J.W.; Naidu, R.; Megharaj, M. Environmental monitoring of the role of phosphate compounds in enhancing immobilization and reducing bioavailability of lead in contaminated soils. *J. Environ. Monit.* **2011**, *13*, 2234–2242. [CrossRef]
6. Derun, E.M.; Demirozu, T.; Piskin, M.B.; Piskin, S. The analysis of corrosion performance of car bodies coated by no nickel and low nickel zinc phosphating processes. *Mater. Corros.* **2005**, *56*, 412–416. [CrossRef]
7. Cubillos, G.I.; Olaya, J.J.; Clavijo, D.; Alfonso, J.E.; Bethencourt, M. Corrosion resistance and biocompatibility of zirconium oxynitride thin film growth by rf sputtering. *Rev. Mex. De Fis.* **2012**, *58*, 328–334.
8. Santos, M.; Freire, C. Evaluation of corrosion resistance of steel coated with zinc-iron alloy electrodeposits containing BTSE, BTESPTS and rare earth salts as conversion films. *Matéria* **2013**, *18*, 1576–1586.
9. Aramaki, K. Protection of zinc from corrosion by coverage with a hydrated cerium(III)oxide layer and ultrathin polymer films of a carboxylate self-assembled monolayer modified with alkyltriethoxysilanes. *Corros. Sci.* **2007**, *49*, 1963–1980. [CrossRef]
10. Liu, M.; Cheng, X.; Li, X.; Liu, G.; Pang, J.; Zhu, Y. Corrosion Behavior of Cr Modified HRB400 Steel Rebar in 2%NaCl Solution. *Corros. Sci. Prot. Technol.* **2015**, *27*, 559–564. (In Chinese)
11. Robin, A.; Silva, G.; Rosa, J.L. Corrosion Behavior of HA-316L SS Biocomposites in Aqueous Solutions. *Mater. Res.* **2013**, *16*, 1254–1259. [CrossRef]
12. Castaneda, A.; Howland, J.J.; Corvo, F.; Perez, T. Corrosion of steel reinforced concrete in the tropical coastal atmosphere of Havana City, Cuba. *Química Nova* **2013**, *36*, 220–229. [CrossRef]
13. Abd el Haleem, S.M.; Ateya, B.G. Cyclic voltammetry of copper in sodium hydroxide solutions. *J. Electroanal. Chem.* **1981**, *117*, 309–319. [CrossRef]
14. Guo, Y.; Chen, Z.; Yin, X.; Yang, W.; Chen, Y.; Liu, Y. Effect of the passive films on $CaCO_3$ scale depositing on Q235 steel: Electrochemical and surface investigation. *J. Colloid Interface Sci.* **2022**, *611*, 172–182. [CrossRef] [PubMed]
15. Xie, Y.; Chen, M.; Xie, D.; Zhong, L.; Zhang, X. A fast, low temperature zinc phosphate coating on steel accelerated by graphene oxide. *Corros. Sci.* **2017**, *128*, 1–8. [CrossRef]
16. Zhang, Z.; Hu, Z.; Singh, P.M. Effects of Chloride Ions on Static and Stress Corrosion Behaviors of 9Cr Martensitic Steel. *Surf. Technol.* **2019**, *48*, 296–303. (In Chinese)
17. Wallinder, D.; Pan, J.; Leygraf, C.; Delblanc-Bauer, A. Eis and XPS study of surface modification of 316LVM stainless steel after passivation. *Corros. Sci.* **1998**, *41*, 275–289. [CrossRef]
18. Lu, J.; Kong, G.; Chen, J.; Xu, Q.; Sui, R. Growth and corrosion behavior of molybdate passivation film on hot dip galvanized steel. *Trans. Nonferrous Met. Soc. China* **2003**, *13*, 145–148.
19. Wang, M.; Ma, R.; Du, A.; Hu, S.; Muhammad, M.; Cao, X.; Fan, Y.; Zhao, X.; Wu, J. Corrosion resistance of black phosphorus nanosheets composite phosphate coatings on Q235 steel. *Mater. Chem. Phys.* **2020**, *250*, 123056. [CrossRef]
20. Al-Refaie, A.A.; Walton, J.; Cottis, R.A.; Lindsay, R. Photoelectron spectroscopy study of inhibition of mild steel corrosion by molybdate and nitrite anions. *Corros. Sci.* **2010**, *52*, 422. [CrossRef]